Improving ambient contrast ratio and color uniformity of mini full color light-emitting diodes using an SiO_2/graphite bi-layered packaging structure

Zong-Tao Li
National & Local Joint Engineering Research Center of Semiconductor Display and Optical Communication Devices, South China University of Technology, Guangzhou 510641, China.
Guangdong Provincial Key Laboratory of Semiconductor Micro Display, Foshan Nationstar Optoelectronics Company Ltd.,
Foshan 528000, China.
meztli@scut.edu.cn

Jun-Hao Wu
National & Local Joint Engineering Research Center of Semiconductor Display and Optical Communication Devices, South China University of Technology, Guangzhou 510641, China.
mejhwu@mail.scut.edu.cn

Zhi-yao Ren
National & Local Joint Engineering Research Center of Semiconductor Display and Optical Communication Devices, South China University of Technology, Guangzhou 510641, China.
201864040304@mail.scut.edu.cn

Yao-xing Song
National & Local Joint Engineering Research Center of Semiconductor Display and Optical Communication Devices, South China University of Technology, Guangzhou 510641, China.
202020100046@mail.scut.edu.cn

Jia-Sheng Li[1]
National & Local Joint Engineering Research Center of Semiconductor Display and Optical Communication Devices, South China University of Technology, Guangzhou 510641, China.

[1] Corresponding author.

Guangdong Provincial Key Laboratory of Semiconductor Micro Display, Foshan Nationstar Optoelectronics Company Ltd.,
Foshan 528000, China.
Jiasli@foxmail.com

ABSTRACT

Mini full-color light-emitting diodes (mini-fc-LEDs) are a promising solution for display applications, including outdoor, cinema, and wearable devices, owing to their high resolution. However, it is difficult to simultaneously obtain high color uniformity and ambient contrast ratio (ACR). To solve this issue, we report a bi-layered packaging structure with an SiO_2 scattering layer on the bottom and a graphite extinction layer on the top. The bi-layered packaging structure combines the scattering effect of SiO_2 nanoparticles and the extinction effect of graphite nanoparticles, wherein the scattering effect improves the color uniformity, and the extinction effect improves the ACR. The color uniformity and ACR of the mini-fc-LEDs were selectively adjusted by changing the nanoparticle concentration and the thickness ratio of the bi-layer. Compared to conventional devices, the inhomogeneity of the bi-layered devices reduced by 65.9%, the ACR increased by 32.9%, and the figure of merit (FOM, representing the overall performance of the device) increased by 168.8%. We believe that the proposed packaging structure can also be applied to other LEDs such as OLEDs and micro-LEDs.

Keywords: mini fc-LEDs, SiO_2 nanoparticles, Graphite nanoparticles, Ambient contrast ratio (ACR) , Inhomogeneity

INTRODUCTION

LEDs offer the advantages of low-voltage drive, high energy utilization, small size, high response speed, environmental protection, and brightness control [1, 2], thereby leading to their widespread usage in various full-color display scenarios [3-5]. Early LED full-color display technology mainly used LEDs as the backlight source of liquid crystal displays (LCDs), which have the advantages of low power consumption, long life, and low

cost [6]. However because LCDs are non-emissive technologies, they suffer from the disadvantages of low contrast ratio, long response time, and narrow color gamut, therefore, cannot achieve high dynamic range (HDR) displays and high quality full-color displays [7, 8]. Organic LEDs (OLEDs) based on organic electroluminescence (EL) make up for these shortcomings of LCDs and achieve full-color displays with higher resolution, faster response, and flexibility [9]. The difficulty of OLEDs mainly lies in the short working life of the blue pixel and the low contrast ratio caused by low peak brightness [10, 11]. In recent years, mini- and micro-LEDs-based full-color display technologies have received widespread attention because of their simple structure, high response speed, and good stability[12]. Mini-LEDs are LEDs with a chip size of 75-300 μm, and micro-LEDs are LEDs with a chip size of less than 75 μm. The extremely small size also guarantees extremely high resolution. Because they can achieve an excellent dark state and the peak brightness is higher than that of LCDs and OLEDs, the contrast ratio of mini- and micro-LEDs is significantly better than that of LCDs and OLEDs, thereby presenting tremendous application prospects of mini- and micro-LEDs in future HDR full-color displays [13, 14]. Owing to the small size of the micro-LEDs, the massive chip transfer process is still in the research stage, and the low-cost mass production cannot be achieved in the short term [15]. The production process of mini-LEDs has been relatively mature, and its performance is better than that of LCDs and OLEDs on the market, so it has the potential to become an emerging display technology.

Similar to OLEDs, mini full-color LEDs (mini-fc-LEDs) also need to further improve the contrast ratio to meet the requirements of HDR high-quality displays. Contrast ratio

calculation, in the traditional sense, uses the ratio of the peak brightness to the minimum brightness of the device itself [16]. Therefore, when improving the contrast ratio, the main consideration is to increase the difference between the peak brightness and the minimum brightness of the device itself, without considering the actual environmental factors and the influence of the device transmittance [17]. In practical applications such as outdoor displays, mobile devices, and wearable display devices, the display quality is affected by ambient light and the transmittance of the device itself [18]. Therefore, the ambient contrast ratio (ACR) is often used to express the performance of the device [19]. To improve ACR, a direct method is to reduce the reflectivity of the device to reduce the reflection of ambient light on the device surface. For example, chemical methods or physical methods can be used to reduce the reflectivity of the device [20]. Jin Hwan Park et al. found that the lactone ring structure would oxidize at low voltage to make the material black [21], and prepared an electrochromic device with controllable ACR and transparency, which improved the display quality of Augmented Reality devices. At the same time, it is also possible to reduce the reflectivity of the device to improve the ACR by adjusting the degree of resonant bonding of the crystal and the alignment of the liquid crystal [22, 23]. Considering the ACR loss that occurs at the oblique angle, a circular polarizer can be used to solve this problem [24].

In addition, mini-fc-LEDs cannot achieve optical color mixing because of the differences in the positions of the red, blue, and green chips, which reduces display quality. In tiny mini-fc-LEDs, color mixing is more sensitive to the difference in position, therefore making color uniformity an urgently needed improvement. The conventional color mixing

methods need to add complex optical elements such as light pipes, diffusers, total internal reflection lenses, and color mixing bars [25-28], which makes the display device is not suitable for mobile display, outdoor display and other applications. In LED packaging, scattering powder can be doped into the encapsulant to scatter light to improve the light distribution [29-32], the radiation power of the device, and the uniformity of correlated color temperature [33-37]. However, the methods that improve the color uniformity and the ACR simultaneously or improve the ACR and the light efficiency simultaneously are rare [38-41], thereby greatly limiting the overall performance improvement of mini-fc-LED displays.

In this study, we propose a bi-layered packaging structure, with a scattering layer on the bottom and an extinction layer on the top, to achieve the simultaneous improvement of the color uniformity and ACR of mini-fc-LEDs. Among them, SiO_2 nanoparticles are doped in the scattering layer to improve color uniformity, and graphite nanoparticles are doped in the extinction layer to improve ACR. The graphite nanoparticles was selected because it is a commonly used material with a high extinction coefficient, which meets the conditions for improving ACR. Furthermore, the influence of the concentration of SiO_2 nanoparticles and graphite nanoparticles on the performance of mini-fc-LEDs with conventional packaging structure was analyzed, and the optical mechanism of these two nanoparticles on mini-fc-LED displays was revealed. Accordingly, an appropriate concentration was selected to prepare mini-fc-LEDs with a bi-layered packaging structure. We analyzed the influence of the particle concentration of the scattering/extinction layer and the thickness ratio of the two layers on the radiation power, inhomogeneity, and ACR

of the device. By optimizing the nanoparticle concentration and thickness ratio of the bi-layered device, mini-fc-LEDs with excellent color uniformity and ACR were prepared.

EXPERIMENTAL

Material Preparation

The mini fc-LEDs used in this study are shown in Fig. 1(a). The substrate size is 2 x 2 mm, the size of the green chip and blue chip is 170 x 120 μm, and the size of the red chip is 130 x 130 μm. The photograph, schematic and SEM image of the prepared mini fc-LEDs with bi-layered packaging structure are shown in Fig. 1(b), (c) and (d). The conventional devices with silicone-only encapsulation is used as the reference device in this study. The scanning electron microscope (SEM) images of the SiO_2 nanoparticles and graphite nanoparticles used in this study are shown in Fig. 1 (e) and (f). The average particle size of the SiO_2 nanoparticles was 136 nm, and that of the graphite nanoparticles was 56 nm. The refractive index of the silicon adhesive, SiO_2 and graphite nanoparticles are 1.40, 1.54 and 2.41, respectively. The CIE chromaticity coordinates of (0.4778, 0.34), (0.1598, 0.1176), (0.0546, 0.3762) corresponding to the red light, blue light, and green light of the mini fc-LEDs are showed in Fig. 1(g). The inset of Fig. 1(g) shows the emission spectrum and chromaticity coordinates of the mini-fc-LEDs, in which the emission peaks of red light, blue light, and green light are 613 nm, 475 nm, and 523 nm, respectively, and the full widths at half maximum (FWHM) are 17 nm, 30 nm, and 20 nm, respectively. To prepare bi-layered mini-fc-LEDs, the mixture of nanoparticles and silicone was first degassed by a vacuum de-aeration machine to obtain SiO_2-doped silicone and graphite-doped silicone. Then, the SiO_2-doped silicone was dispensed into the device package and cured at 150 °C

for 3 h, and then the graphite-doped silicone was dispensed into the same device package and cured at 150 °C for 3 h. The thickness ratio of the scattering layer to the extinction layer is changed by controlling the amount of SiO_2-doped silicone and graphite-doped silicone, the total dispensing amount of the encapsulant was 1.2 mg. After the device is completely curing, the thickness ratio of the scattering layer to the extinction layer is obtained from the cross-sectional view of the device. To characterize the optical performance of the device, the film was prepared using a scraper coating machine. The reflectivity, transmittance, and haze of the film were measured using an ultraviolet spectrophotometer. The radiant power and spatial intensity distributions of the devices were tested by an integration system under the working conditions of 10 mA and 3 V (rated working conditions).

Parameter Characterization

ACR is an important parameter of display devices, and its definition is as follows[42]:

$$ACR = \frac{L_{\text{on}} + RL_{\text{ambient}}}{0 + RL_{\text{ambient}}}, \quad (1)$$

where L_{on} is the brightness of the device when it is working, $L_{ambient}$ is the ambient brightness, *and R* is the reflection coefficient. The calculation formula is

$$R = \frac{\int_{400}^{760} V(\lambda)S(\lambda)R(\lambda)\mathrm{d}(\lambda)}{\int_{400}^{760} V(\lambda)S(\lambda)\mathrm{d}(\lambda)}, \quad (2)$$

where $V(\lambda)$ represents the human eye sensitivity function, $R(\lambda)$ is the spectral reflectance of the device, and $S(\lambda)$ is the spectrum of the ambient light (the CIE standard D65 light source spectrum is used in this study).

This study uses non-uniformity to quantify color uniformity [26]. We measure the spatial intensity distributions of the red, green, and blue LED chips, and then calculated the sum of the dispersion among these distributions, which is defined as inhomogeneity I_0. A smaller inhomogeneity demonstrates better color uniformity of the device. For convenience, we take ninety points on each spatial intensity distribution and mark them as R(i), G(i), and B(i) for red, blue, and green light, respectively. Therefore, the inhomogeneity is defined as

$$I_0 = \sum_{i=1}^{90} （|R(i) - G(i)| + |R(i) - B(i)| + |G(i) - B(i)|）, 1 \leqslant i \leqslant 90 \quad (3)$$

RESULTS AND DISCUSSION

To study the scattering effect of SiO_2 nanoparticles and the extinction effect of graphite nanoparticles, SiO_2-only devices with a SiO_2 concentration ranging from 0 to 50 wt% and graphite-only devices with graphite concentrations ranging from 0 to 0.4 wt% were prepared. The ambient contrast ratio (ACR) of SiO_2-only devices with different SiO_2 concentrations and graphite-only devices with different graphite concentrations are shown in Fig. 2(a). The ACR of the SiO_2-only devices decreased slightly with increasing SiO_2 concentration, and dropped below 100 when the ambient light was greater than 100 lux. This demonstrates that the increase in the SiO_2 concentration does not help increase the ACR of the SiO_2-only devices, and the reasons are explained subsequently. Fig. 2(b) shows the radiation power of the SiO_2-only devices with different SiO_2 concentrations, in which the radiation power proportion is the percentage of the SiO_2-only devices/graphite-only devices relative to the conventional device. As the SiO_2 concentration increased, the

radiation power increased and reached a maximum at a SiO_2 concentration of 2.4 wt%, which is 6.7% higher than that of the conventional devices. This is because light with a large emission angle from chips is susceptible to scattering due to the long light path in the encapsulant. This means that a portion of light with a large emission angle can be converted into a small emission angle, and then escape from the device with less Fresnel loss or total internal reflection. As the SiO_2 concentration further increased, the radiation power of the SiO_2-only devices decreased, owing to the stronger backscattering effect, while it still maintains over 60% of the radiation power of the conventional devices. In addition, the scattering effect of SiO_2 nanoparticles can also significantly reduce the inhomogeneity of the SiO_2-only devices, as shown in Fig. 2 (c). The inhomogeneity of the SiO_2-only devices decreased with an increase in the SiO_2 concentration, and the lowest value was obtained when the SiO_2 concentration was 25 wt%. From the sub-figures in Fig. 2(c), it is evident that the red, green, and blue spatial intensity distributions of mini-fc-LEDs tend to be consistent with increasing SiO_2 concentration. These results demonstrate that the color uniformity of SiO_2-only devices improved owing to the stronger scattering effect of SiO_2 nanoparticles. Furthermore, when the SiO_2 concentration was greater than 25 wt%, the inhomogeneity increased as the SiO_2 concentration continued to increase, indicating that the scattering effect had a critical point in reducing the inhomogeneity. A more detailed discussion of the critical point is provided in the subsequent section.

As for the graphite-only devices, their ACR increased significantly as the graphite concentration increased, as shown in Fig. 2(a). For example, the ACR of the graphite-only devices with a graphite concentration of 0.4 wt% was 942.9 at an ambient brightness of

100 lux, which is 989.4% higher than that of conventional devices. Therefore, a larger graphite concentration proved more beneficial for eliminating the influence of ambient light. Figs. 2(d) and (e) show the radiation power and inhomogeneity of graphite-only devices, respectively. With the increase in the graphite concentration, the radiation power of the graphite-only devices dropped sharply, i.e., only 3.0% of the radiation power remained at a graphite concentration of 0.4 wt%. This means that the reduction in radiation power cannot be neglected when using graphite nanoparticles to improve the ACR of the devices. Therefore, the graphite concentration was subsequently selected to be lower than 0.4 wt%. The graphite concentration also influenced the inhomogeneity of the devices, which can be divided into three phases, as shown in Fig. 2 (e). In phase I, the low graphite concentration led to a weak extinction effect, and graphite nanoparticles in this phase were mainly used as scattering particles to slightly reduce the inhomogeneity of the graphite-only devices. In phase II, as the graphite concentration further increased, the extinction effect gradually became stronger, with the graphite nanoparticles exhibited a high probability to absorb light. In addition, the light scattered by graphite nanoparticles led to a long optical path, contributing to much more extinction events. This means that the uniform light distribution formed by the scattering effect was destroyed by the extinction effect, which increased the inhomogeneity. In phase III, when the graphite concentration was too high, the light with a large emission angle and light after multiple scattering was absorbed completely because of the long light path. It reduced the influence of stray light on the light distribution, so the light was concentrated in an area with a small emission angle to slightly reduce the inhomogeneity. These results show that

although doping graphite nanoparticles in mini-fc-LED packaging can greatly improve the ACR of the devices, it significantly reduces the radiation power and cannot reduce the inhomogeneity.

From the previous discussion, it is demonstrable that the doping of SiO_2 nanoparticles in the encapsulant can effectively reduce the inhomogeneity of mini fc-LEDs, while the doping of graphite nanoparticles can significantly improve the ACR. To ascertain the mechanism of these phenomena, SiO_2-only films with a SiO_2 concentration range of 0-50 wt% and graphite-only films with a graphite concentration range of–0-0.4 wt% were prepared, both of which had a thickness of 0.5 mm (the value is equivalent to the encapsulant thickness of the SiO_2-only devices and graphite-only devices). Fig. 3 shows the reflectivity, transmittance, and haze of the SiO_2-only films and the graphite-only films, which were tested using an ultraviolet spectrophotometer. The photographs of SiO_2-only films are shown in Fig. 3 (a), where the visible light transmittance decreased as the SiO_2 concentration increased. Fig. 3 (b) shows that when the SiO_2 concentration increased in the interval of 0-25 wt%, the transmittance of the SiO_2-only films decreased slightly, which corresponds to the slight reduction in the radiation power of the SiO_2-only devices in Fig. 2. The haze of SiO_2-only films increased significantly as the SiO_2 concentration increased in the interval of 0-25 wt%, which corresponds to a significant reduction in inhomogeneity of the SiO_2-only devices in Fig. 2. This means that the scattering effect of SiO_2 nanoparticles is the reason why the spatial intensity distributions of SiO_2-only devices become uniform. It can be observed that the decrease in transmittance was nearly equal to the increase in haze as the SiO_2 concentration increased in the interval of 25-50 wt%.

Therefore, the amount of scattered light, which is defined as the value of transmittance multiplied by haze, hardly changed in the SiO_2 concentration interval of 25 -50 wt%. This demonstrates that the scattering effect of the SiO_2 nanoparticles was saturated when the SiO_2 concentration was 25 wt%. When the SiO_2 concentration was greater than 25 wt%, multi-scattering and severe total internal reflection destroyed the uniform spatial intensity distributions of the SiO_2-only devices, which reasonably explains why the inhomogeneity of SiO_2-only devices achieved a minimum at the SiO_2 concentration of 25 wt%. Fig. 3(c) shows photographs of the graphite-only films with different graphite concentrations, where a strong visible light extinction was observed at a high graphite concentration. Fig. 3(d) shows the transmittance and haze of graphite-only films with different graphite concentrations. The transmittance of the graphite-only films decreased sharply and the haze increased slightly as the graphite concentration increased, which means that the amount of scattered light was less. This shows that the graphite nanoparticles mainly play a role of extinction rather than scattering in the encapsulant, which is consistent with the results of the poor color uniformity and excellent ACR of the graphite-only devices in Fig. 2.

Fig. 3(e) shows the visible light reflectance spectrum of SiO_2-only films and graphite-only films. The reflectivity of SiO_2-only films increased monotonically as the SiO_2 concentration increased, at most 24.6% higher than that of the 0 wt% films. This is because the ambient light is reflected by the scattering effect, which is similar to total internal reflection. It is worth noting that the reflectivity of the SiO_2-only films with a SiO_2 concentration of 25 wt% and a SiO_2 concentration of 50 wt% was very close, indicating

that the scattering effect was saturated when the SiO_2 concentration was 25 wt%. As for the graphite-only films, their reflectivity decreased monotonously as the graphite concentration increased, at most 44.4% lower than that of the 0 wt% films. It can be inferred that the scattering effect of the SiO_2 nanoparticles increased the reflectivity of the SiO_2-only devices, reducing the ACR of the devices, while the strong extinction effect of the graphite nanoparticles reduced the reflectivity of the graphite-only devices, thereby increasing the ACR of the devices.

Based on the above discussion, the inhomogeneity of mini fc-LEDs was reduced by doping with SiO_2 nanoparticles in the encapsulant, which slightly reduced the ACR of the devices simultaneously, as shown in Fig. 4(a). Doping graphite nanoparticles in the encapsulant can greatly increase the ACR of mini fc-LEDs, which seriously reduced the radiation power and the color uniformity of the devices, as shown in Fig. 4(b). The advantages and disadvantages of SiO_2 nanoparticles and graphite nanoparticles are complementary, so the advantages of the two nanoparticles can be combined through a suitable packaging structure. In the discussion of graphite-only devices in Fig. 2, it is proven that the scattering effect will extend the optical path, which causes more light to become extinct by the extinction effect. Therefore, a device with high ACR and low inhomogeneity cannot be obtained by simply doping SiO_2 nanoparticles and graphite nanoparticles simultaneously. Consequently, this study designs a bi-layered packaging structure to combine the advantages of SiO_2 nanoparticles and graphite nanoparticles.

From the previous analysis, the scattering effect of SiO_2 nanoparticles will increase the reflectivity of the devices, while the extinction effect of graphite nanoparticles will

cause a sharp drop in the transmittance of the devices. Therefore, if the bi-layered packaging structure has a scattering layer on top and an extinction layer on the bottom, as shown in Fig. 4(c), most of the ambient light will be reflected on the scattering layer, which reduces the ACR of the devices. Meanwhile, most of the light emitted by the chips was extinct in the extinction layer, and only a small part of the light was scattered in the scattering layer for color mixing. The color uniformity improvement effect was not as good as when a large amount of light was scattered. If the bi-layered packaging structure has a scattering layer on the bottom and the extinction layer on the top, as shown in Fig . 4(d), the above problems can be avoided. The ambient light will be mostly extinct in the top extinction layer, which effectively improves the ACR of the devices. A large amount of light emitted by the chip was fully scattered in the bottom scattering layer, which improved the color uniformity improvement effect. Therefore, a bi-layered packaging structure with a bottom scattering layer and a top extinction layer was used for subsequent studies.

By fixing the SiO_2 concentration of the scattering layer, we studied the optical performance of the bi-layered mini-fc-LEDs by changing the graphite concentration of the extinction layer and the thickness ratio of the scattering layer to the extinction layer. Similar to the previous study, the bi-layered devices and films were prepared to test the performance, and the results are shown in Fig. 5, where the thickness ratio refers to the value of the scattering layer thickness divided by the extinction layer thickness. According to the discussion of SiO_2-only devices in Fig. 2, the SiO_2-only devices with 25 wt% SiO_2 concentration had the best color uniformity and the preferable radiation power

proportion (71.2%). Therefore, 25 wt% was selected as the SiO_2 concentration of the scattering layer, and the graphite concentration of the extinction layer ranged from 0 to 0.4 wt%. As the graphite concentration increased and the thickness ratio decreased, the ACR of the bi-layered devices increased significantly, as shown in Fig. 5 (a), while the radiation power of the bi-layered devices decreased significantly, as shown in Fig. 5(b). Increasing the graphite concentration or reducing the thickness ratio actually increased the graphite nanoparticle content in the device encapsulant, i.e., it enhanced the extinction effect of the extinction layer. The transmittance and reflectivity of the bi-layered films were tested, and the results are shown in Fig. 5(c) and (d). The transmittance and reflectivity of the bi-layered films decreased as the graphite concentration increased and the thickness ratio decreased, indicating that the extinction effect of the extinction layer was the key factor affecting the ACR and the radiation power of the bi-layered devices. These results show that the scattering layer does not affect the extinction effect of the extinction layer in the bi-layered devices.

The inhomogeneity of the bi-layered devices is shown in Fig. 5 (e). Except for the device with a thickness ratio of 5:1, the inhomogeneity of the bi-layered devices with other thickness ratios initially exhibited a decreasing trend and then increased as the graphite concentration of the extinction layer increased. The minimum of inhomogeneity were obtained at the graphite concentration of 0.05 wt% (thickness ratio is 2:1 and 3:1) and 0.1 wt% (thickness ratio is 1:1). Similar to the case of graphite-only devices in Fig. 2(e), when the graphite concentration of the extinction layer was low, the graphite nanoparticles reduced the inhomogeneity to a small extent by scattering. When the

graphite concentration of the extinction layer was high, the inhomogeneity increased due to the mixed effect of extinction and scattering. However, when the thickness ratio was 5:1, the extinction layer was too thin to reduce inhomogeneity by scattering. Therefore, the inhomogeneity increased monotonically with the increase in the graphite concentration as the thickness ratio approached 5:1. In the case of 0 wt% graphite concentration, the inhomogeneity of the bi-layered devices dropped from 13.4 to 7.7 as the thickness ratio increased, which was higher than the inhomogeneity of the SiO_2-only devices with 25 wt% SiO_2 concentration (5.5). It is worth noting that when the thickness ratio was 5:1, the scattering layer thickness of the bi-layered devices was close to the encapsulant thickness of the SiO_2-only devices, but the inhomogeneity between the two devices was significantly different. This means that the scattering effect of the scattering layer was affected by the extinction layer and the Fresnel refraction between the two layers, causing an increase in the thickness of the scattering layer that could only slightly reduce the inhomogeneity. To determine the relationship between the inhomogeneity and the graphite concentration of the extinction layer, the haze of the bi-layered films was tested, as shown in Fig. 5 (f). The haze of the bi-layered films was almost unchanged as the graphite concentration increased, which demonstrates that the extinction layer only slightly interfered with the scattering effect of the scattering layer and then affected the spatial intensity distributions of the bi-layered devices to a small extent. However, the inhomogeneity of the bi-layered devices is sensitive to the spatial intensity distributions, which results in the fact that although the haze of the bi-layered films was basically unchanged, the inhomogeneity of the bi-layered devices was greatly affected as the

graphite concentration increased

According to the above analysis, the extinction layer weakens the effect of the scattering layer on improving the color uniformity. Subsequently, this weakening was compensated by changing the SiO_2 concentration of the scattering layer, when the thickness ratio and the top graphite concentration were fixed. The figure of merit (FOM) was introduced to select the thickness ratio and the top graphite concentration, defined as

$$FOM = \frac{F*A}{I}, \quad (4)$$

where *F*, *A*, and *I* are the normalized radiation power, ACR (device brightness is 1500 nits and the ambient brightness is 50 lux) and inhomogeneity, respectively. FOM is a comprehensive evaluation of radiation power, inhomogeneity, and ACR. A higher FOM indicates a better comprehensive performance of the device. The FOM calculation results are listed in Table 1.

According to Table 1, devices A and B are preferred, while device A has lower inhomogeneity and device B has better ACR. In the discussion on SiO_2-only devices, it has been proved that the SiO_2 nanoparticles predominantly affect the inhomogeneity of the devices rather than the ACR. Therefore, a device with a higher ACR should be selected in this section, in which the inhomogeneity can be further improved by changing the SiO_2 concentration. Consequently, the configuration of device B was used in this section, i.e., the graphite concentration of the extinction layer was 0.1 wt% and the thickness ratio was 2:1. Subsequent research was carried out in this configuration.

The ACR of the bi-layered devices reduced slightly when the SiO_2 concentration of

the scattering layer increased, as shown in Fig. 6 (a). Therefore, the SiO_2 concentration of the scattering layer is not an important factor affecting the ACR of bi-layered devices. As shown in Fig. 6 (b), the inhomogeneity of the bi-layered devices decreased monotonically with an increase in the SiO_2 concentration, reaching 5.8 at 40 wt% SiO_2 concentration, which is close to the inhomogeneity of the SiO_2-only devices with 25 wt% SiO_2 concentration(5.5). Unlike SiO_2-only devices, increasing the SiO_2 concentration of the scattering layer in the range of 25 wt% to 40 wt% did not increase the inhomogeneity of the bi-layered devices. This is because the scattering layer thickness of the bi-layered devices was lower than that of the SiO_2-only devices, so a higher SiO_2 concentration was required in the bi-layered devices to achieve the same saturated state. Fig. 6 (c) shows that the radiation power of the bi-layered devices increased slightly and then decreased as the SiO_2 concentration increased. The transmittance of the bi-layered films decreased slightly and the haze increased with the enhancement of the SiO_2 concentration as shown in Fig. 6(d). The trends of the bi-layered devices in ACR, radiation power, haze, and transmittance were both similar to those of the SiO_2-only devices. Therefore, we conclude that the extinction layer only weakens the reduction effect of the scattering layer on the inhomogeneity of the bi-layered devices, and this weakening can be compensated by increasing the SiO_2 concentration of the scattering layer within a certain range. This means that the SiO_2 concentration is an important factor determining the inhomogeneity of the bi-layered devices.

In summary, it is feasible to obtain a device with a good ACR and inhomogeneity by combining the scattering effect of SiO_2 nanoparticles and the extinction effect of graphite

nanoparticles through a bi-layered packaging structure. To compare the optical performance of devices with different packaging structures, Table 2 lists the optical performance of four devices with different packaging structures. Compared to the SiO_2-only devices, the inhomogeneity of the bi-layered devices only increased by 5.5%, but ACR increased by 96.1%. Compared to the graphite-only devices, the ACR of the bi-layered devices dropped by 54.9%, but the inhomogeneity dropped by 74.9%. Compared to conventional devices, the inhomogeneity of the bi-layered devices decreased by 65.9%, and ACR increased by 32.9%. The FOM of the bi-layered device was 168.8%, 89.7%, and 130.1% higher than those of conventional devices, SiO_2-only devices, and graphite-only devices, respectively. The calculation result of the FOM shows that the overall performance of the bi-layered device is the best.

CONCLUSIONS

In this study, a bi-layered packaging structure combining extinction and scattering was introduced to simultaneously improve the ACR and the inhomogeneity of the mini-fc-LEDs. According to the discussion on SiO_2-only devices and graphite-only devices, the inhomogeneity of mini-fc-LEDs significantly improved due to the scattering effect of SiO_2 nanoparticles, while it also increased the reflectivity of the SiO_2-only devices, resulting in a reduction in the ACR. In the SiO_2-only devices, the scattering effect of the SiO_2 nanoparticles was saturated as the SiO_2 concentration was greater than 25 wt%. The extinction effect of graphite nanoparticles can greatly reduce the reflectivity of the graphite-only devices and improve the ACR, while resulting in low radiation power and

high inhomogeneity. To combine the advantages of the two kinds of nanoparticles, we carefully designed a bi-layered packaging structure with a scattering layer on the bottom and an extinction layer on the top. We demonstrated that the scattering layer did not affect the extinction effect of the extinction layer; in fact, the extinction layer weakened the reduction effect of the scattering layer on the inhomogeneity, which can be compensated by increasing the SiO_2 concentration of the scattering layer. The decisive factors affecting the radiation power and ACR of the bi-layered devices were the graphite concentration and thickness of the extinction layer, while the decisive factors affecting the inhomogeneity of the bi-layered devices were the SiO_2 concentration of the scattering layer. According to the FOM, the graphite concentration, SiO_2 concentration, and thickness ratio of the bi-layered devices were optimized to be 0.1 wt%, 40 wt%, and 2:1, respectively. The results showed that the FOM of the optimized bi-layered devices was 168.8%, 89.7%, and 130.1% higher than that of conventional devices, SiO_2-only devices (SiO_2 concentration of 25 wt%), and graphite-only devices (graphite concentrations of 0.1 wt%) respectively, which proves that the bi-layered packaging structure can achieve excellent comprehensive performance. This discovery can also contribute to display applications of other LED devices, including micro-LEDs, OLEDs, and quantum dot-LEDs.

FUNDING

This work was supported by the Natural Science Foundation of Guangdong Province(No. 2018B030306008), the National Natural Science Foundation of China(No. 51775199),

the National Natural Science Foundation of China(No. 51735004), and the Fundamental Research Funds for the Central Universities.

REFERENCES

[1] Pust P., Schmidt P. J., and Schnick W., 2015, "A revolution in lighting," Nature Materials, 14(5), pp. 454-458.

[2] Yuan F., Yuan T., Sui L., Wang Z., Xi Z., Li Y., Li X., Fan L., Tan Z., Chen A., Jin M., and Yang S., 2018, "Engineering triangular carbon quantum dots with unprecedented narrow bandwidth emission for multicolored LEDs," Nat Commun, 9(1), p. 2249.

[3] Hyot B., Roll è s M., and Miska P., 2019, "Design of Efficient Type - II ZnGeN2/In0.16Ga0.84N Quantum Well - Based Red LEDs," physica status solidi (RRL) – Rapid Research Letters, 13(8), p. 1900170.

[4] Emmel J., and Whitehead L. A., 2013, "Modified point spread function for efficient high dynamic range LED backlight capable of high uniformity, high contrast, and smooth gradients," Appl Opt, 52(34), pp. 8239-8244.

[5] Nakamura S., Mukai T., and Senoh M., 1994, "Candela - class high - brightness InGaN/AlGaN double - heterostructure blue - light - emitting diodes," Applied Physics Letters, 64(13), pp. 1687-1689.

[6] Chen H., and Wu S.-T., 2019, "Advanced liquid crystal displays with supreme image qualities," Liquid Crystals Today, 28(1), pp. 4-11.

[7] Su F.-M., and Su C.-T., 2020, "TFT-LCD Contrast Ratio Improvement by Using Design for Six Sigma Disciplines," IEEE Transactions on Semiconductor Manufacturing, 33(1), pp. 128-139.

[8] Luo Z., Xu D., and Wu S.-T., 2014, "Emerging Quantum-Dots-Enhanced LCDs," Journal of Display Technology, 10(7), pp. 526-539.

[9] Chen H. W., Lee J. H., Lin B. Y., Chen S., and Wu S. T., 2018, "Liquid crystal display and organic light-emitting diode display: present status and future perspectives," Light Sci Appl, 7, p. 17168.

[10] Ashok Kumar S., Shankar J. S., K Periyasamy B., and Nayak S. K., 2019, "Device engineering aspects of Organic Light-Emitting Diodes (OLEDs)," Polymer-Plastics Technology and Materials, 58(15), pp. 1597-1624.

[11] Yang X., Xu X., and Zhou G., 2015, "Recent advances of the emitters for high performance deep-blue organic light-emitting diodes," Journal of Materials Chemistry C, 3(5), pp. 913-944.

[12] Huang Y., Tan G., Gou F., Li M.-C., Lee S.-L., and Wu S.-T., 2019, "Prospects and challenges of mini-LED and micro-LED displays," Journal of the Society for Information Display, 27(7), pp. 387-401.
[13] Bartczak K., Walczak A., Jander S., Zwoliński R., Banyś A., Ammer A., Wranicz J. K., and Jaszewski R., 2013, "Implantation of an epicardial lead through minithoracotomy as an alternative for patients with leadrelated endocarditis who require permanent pacing," Polish Journal of Cardio-Thoracic Surgery, 1, pp. 62-66.
[14] Li Z.-T., Cao K., Li J.-S., Tang Y., Xu L., Ding X.-R., and Yu B.-H., 2019, "Investigation of Light-Extraction Mechanisms of Multiscale Patterned Arrays With Rough Morphology for GaN-Based Thin-Film LEDs," IEEE Access, 7, pp. 73890-73898.
[15] Wong M. S., Nakamura S., and DenBaars S. P., 2019, "Review—Progress in High Performance III-Nitride Micro-Light-Emitting Diodes," ECS Journal of Solid State Science and Technology, 9(1), p. 015012.
[16] Yoon C., and Choi J.-h., 2014, "Synthesis of tricyanopyrrolidone derivatives as synergists for improving contrast ratio of liquid crystal displays," Dyes and Pigments, 101, pp. 344-350.
[17] Kim S.-H., Yun S., Choi J., and Kim J. H., 2018, "High contrast fluorescence switching based on CH3NH3PbBr3 perovskite nanoparticles in photochromic composites," Journal of Photochemistry and Photobiology A: Chemistry, 353, pp. 279-283.
[18] Hwang A. D., and Peli E., 2016, "New Contrast Metric for Realistic Display Performance Measure," Digest of technical papers. SID International Symposium, 47(1), pp. 982-985.
[19] Chen H., Tan G., and Wu S.-T., 2017, "Ambient contrast ratio of LCDs and OLED displays," Optics Express, 25(26), p. 33643.
[20] Ik Jang K., Jin Hwan P., Yong Cheol K., Gyeong Woo K., and Jang Hyuk K., 2017, "High optical contrast reflective display with electrochromism," SID Symposium Digest of Technical Papers, 48(1), pp. 1781-1784.
[21] Jin Hwan P., Yong Cheol K., Ik Jang K., Gyeong Woo K., and Jang Hyuk K., 2017, "High Contrast Ratio Electrochromic Light Shutter Device for Optical See-through Type Head Mounted Display," SID Symposium Digest of Technical Papers, 48(1), pp. 677-680.
[22] Koch C., Schienke G., Paulsen M., Meyer D., Wimmer M., Volker H., Wuttig M., and Bensch W., 2017, "Investigating the Influence of Resonant Bonding on the Optical Properties of Phase Change Materials (GeTe)xSnSb2Se4," Chemistry of Materials, 29(21), pp. 9320-9327.
[23] Chaudhary A., Klebanov M., and Abdulhalim I., 2017, "Liquid crystals alignment with PbS nanosculptured thin films," Liquid Crystals, 45(1), pp. 3-10.
[24] Haiwei C., Guanjun T., and Shin-Tson W., 2018, "Can LCDs Outperform OLED Displays in Ambient Contrast Ratio?," SID Symposium Digest of Technical Papers, 49(1), pp. 981-984.
[25] Son C.-G., Yi J.-H., Gwag J.-S., Kwon J.-H., and Park G.-J., 2011, "Improvement of Color and Luminance Uniformity of the Edge-Lit Backlight Using the RGB LEDs," Journal of the Optical Society of Korea, 15(3), pp. 272-277.

[26] Wang H. C., Chiang Y. T., Lin C. Y., Lu M. Y., Lee M. K., Feng S. W., and Kuo C. T., 2016, "All-reflective RGB LED flashlight design for effective color mixing," Opt Express, 24(5), pp. 4411-4420.

[27] Yang J., Liu Z., Xue B., Liao Z., Feng L., Zhang N., Wang J., and Li J., 2018, "Highly Uniform White Light-Based Visible Light Communication Using Red, Green, and Blue Laser Diodes," IEEE Photonics Journal, 10(2), pp. 1-8.

[28] Blankenbach K., Hertlein F., and Hoffmann S., 2020, "Advances in automotive interior lighting concerning new LED approach and optical performance," Journal of the Society for Information Display, 28(8), pp. 655-667.

[29] Chen K. J., Han H. V., Chen H. C., Lin C. C., Chien S. H., Huang C. C., Chen T. M., Shih M. H., and Kuo H. C., 2014, "White light emitting diodes with enhanced CCT uniformity and luminous flux using ZrO2 nanoparticles," Nanoscale, 6(10), pp. 5378-5383.

[30] Luo X., Hu R., Liu S., and Wang K., 2016, " Heat and Fluid Flow in High-Power LED Packaging and Applications, " Progress in Energy and Combustion Science, 56, pp. 1-32.

[31] Yu X., Hu R., Wu R., Xie B., Zhang X., and Luo X., 2019, "Cylindrical Tuber Encapsulant Layer Realization by Patterned Surface for Chip-on-Board Light-Emitting Diodes Packaging," Journal of Electronic Packaging, 141(3), p.031005..

[32] Li J. S., Tang Y., Li Z. T., Li J. X., Ding X. R., Yu B. H., Yu S. D., Ou J. Z., and Kuo H. C., 2021, "Toward 200 Lumens per Watt of Quantum-Dot White-Light-Emitting Diodes by Reducing Reabsorption Loss," ACS Nano, 15(1), pp. 550-562.

[33] Zhu Y., Chen W., Hu J., Xie B., Hao J., Wu D., Luo X., and Wang K., 2016, "Light Conversion Efficiency Enhancement of Modified Quantum Dot Films Integrated With Micro SiO2Particles," Journal of Display Technology, 12(10), pp. 1152-1156.

[34] Li Z., Song C., Li J., Liang G., Rao L., Yu S., Ding X., Tang Y., Yu B., Ou J., Lemmer U., and Gomard G., 2020, "Highly Efficient and Water‐Stable Lead Halide Perovskite Quantum Dots Using Superhydrophobic Aerogel Inorganic Matrix for White Light‐Emitting Diodes," Advanced Materials Technologies, 5(2), p. 11.

[35] Li Z., Liang J., Li J., Li J., and Tang Y., 2020, "Scattering Nanoparticles-Induced Reflection Effect for Enhancing Optical Efficiency of Inverted Quantum Dots-LEDs Combined with the Centrifugation Technique," J Electronic Packaging, 143(2), p. 021002.

[36] Tang Y., Li Z., Li Z.-T., Li J.-S., Yu S.-D., and Rao L.-S., 2018, "Enhancement of Luminous Efficiency and Uniformity of CCT for Quantum Dot-Converted LEDs by Incorporating With ZnO Nanoparticles," IEEE Transactions on Electron Devices, 65(1), pp. 158-164.

[37] Yu X., Pei N., Zhou S., Zhang X., and Luo X., 2019, "Enhancing Light Efficiency and Moisture Stability of the Quantum Dots-Light-Emitting Diodes by Coating Superhydrophobic Nanosilica Particles," IEEE Transactions on Electron Devices, 66(12), pp. 5196-5201.

[38] Shun-Chieh H., Yin-Han C., Zong-Yi T., Hau-Vei H., Shih-Li L., Teng-Ming C., Hao-Chung K., and Chien-Chung L., 2015, "Highly Stable and Efficient Hybrid Quantum Dot Light-Emitting Diodes," IEEE Photonics Journal, 7(5), pp. 1-10.

[39] Xie B., Hu R., Yu X., Shang B., Ma Y., and Luo X., 2016, "Effect of Packaging Method on Performance of Light-Emitting Diodes With Quantum Dot Phosphor," IEEE Photonics Technology Letters, 28(10), pp. 1115-1118.

[40] Chen S., Yan C., Tang Y., Li J., Ding X., Rao L., and Li Z., 2018, "Improvement in Luminous Efficacy and Thermal Performance Using Quantum Dots Spherical Shell for White Light Emitting Diodes," Nanomaterials (Basel), 8(8),p. 618.

[41] Xie B., Cheng Y., Hao J., Yu X., Shu W., Wang K., and Luo X., 2018, "White Light-Emitting Diodes With Enhanced Efficiency and Thermal Stability Optimized by Quantum Dots-Silica Nanoparticles," IEEE Transactions on Electron Devices, 65(2), pp. 605-609.

[42] Singh R., Narayanan Unni K. N., Solanki A., and Deepak, 2012, "Improving the contrast ratio of OLED displays: An analysis of various techniques," Optical Materials, 34(4), pp. 716-723.

Figure Captions List

Fig. 1 Structures and color gamut of mini-fc-LEDs with bi-layered packaging structures. (a) Photograph of the mini-fc-LEDs without packaging. (b) Photographs, (c) schematic and (d) SEM image of cross-sectional views of mini-fc-LEDs with bi-layered packaging structure. The red dashed line is the boundary between the scattering layer and the extinction layer. (e) SEM image of SiO_2 nanoparticles. The inset shows the particle size distribution with an average size of 136 nm. (f) SEM image of graphite nanoparticles. The inset shows the particle size distribution with an average size of 56 nm. (g) CIE chromaticity coordinates and color gamut (red line) of the mini-fc-LEDs. The inset shows normalized luminescence spectrum of the mini-fc-LEDs.

Fig. 2 Effects of doped nanoparticles on the optical performances of SiO_2-only devices and graphite-only devices. **(a)** Ambient contrast ratio (device brightness is 1500 nits) of device with different nanoparticle concentrations: upper, SiO_2 nanoparticles; lower, graphite nanoparticles. The inset shows the details of Fig. 2. (a). **(b)** Radiation power of SiO_2-only devices with different SiO_2 concentration. **(c)** Inhomogeneity of SiO_2-only devices with different SiO_2 concentration. The inset shows the spatial light distribution curves of the red, blue, and green light corresponding to the

degree of inhomogeneity. **(d)** Radiation power of graphite-only devices with different graphite concentration. **(e)** Inhomogeneity of graphite-only devices with different graphite concentration. In Fig. 2. (b) and (d), the radiation power proportion is the percentage of the SiO_2-only devices/graphite-only devices relative to the conventional device.

Fig. 3 Effects of doped nanoparticles on the optical performances of films. (a) Photograph of SiO_2-only films with different SiO_2 concentration. (b) Transmittance and haze of SiO_2-only films with different SiO_2 concentration. (c) Photograph of graphite-only films with different graphite concentration. (d) Transmittance and haze of graphite-only films with different graphite concentration. (e) Visible light reflectance spectrum of SiO_2-only films (solid lines) and graphite-only films (dashed lines).

Fig. 4 The structure and effect of different bi-layered devices. **(a)** The SiO_2-only device **(b)** The graphite-only device **(c)** The bi-layered device with a top scattering layer and a bottom extinction layer. **(d)** The bi-layered device with a top extinction layer and a bottom scattering layer.

Fig. 5 Effects of graphite concentration of top extinction layer and thickness ratio on the optical performances of bi-layered devices and bi-layered

films. **(a)** ACR (device brightness is 1500 nits and the ambient brightness is 50 lux), **(b)** radiation power and **(d)** inhomogeneity of bi-layered devices with different graphite concentration and different thickness ratio. **(c)**Transmittance, **(e)** reflectivity and **(f)** haze of bi-layered films with different graphite concentration and different thickness ratio. In (a)-(f), the blue dashed line represents the performance of the conventional devices or films; the red dashed line represents the performance of the SiO_2-only device or films (SiO_2 concentration is 25 wt%); the blue dashed line represents the performance of the graphite-only device or films (graphite concentration is 0.4 wt%). All the SiO_2 concentration of the bottom scattering layer is 25 wt%; the thickness ratio refers to the value of the thickness of the scattering layer divided by the thickness of the extinction layer.

Fig. 6 Effects of SiO_2 concentration on performance of bi-layered devices. **(a)** ACR (device brightness is 1500 nits), **(b)** inhomogeneity and **(c)** radiation power of bi-layered devices with different SiO_2 concentration. **(d)** Transmittance and haze of bi-layered films with different SiO_2 concentration. In (a)-(d), the blue dashed line represents the performance of the conventional devices or films; the red dashed line represents the performance of the SiO_2-only devices or films (SiO_2 concentration is 25

wt%); the blue dashed line represents the performance of the graphite-only devices or films (graphite concentration is 0.4 wt%). All the graphite concentration of top extinction layer is 0.1 wt% and the thickness ratio is 2:1.

Table Caption List

Figures

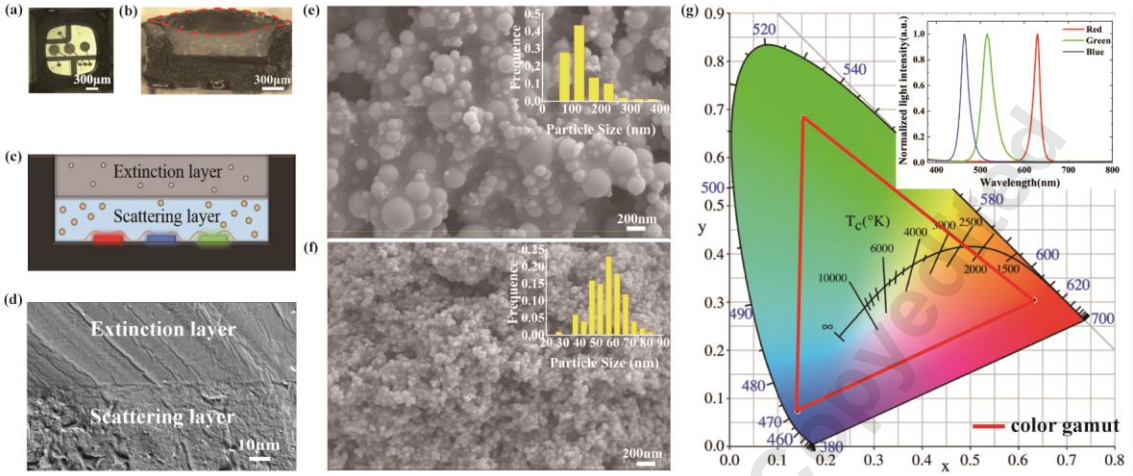

Figure 1. Structures and color gamut of mini-fc-LEDs with bi-layered packaging structures. (a) Photograph of the mini-fc-LEDs without packaging. (b) Photographs, (c) schematic and (d) SEM image of cross-sectional views of mini-fc-LEDs with bi-layered packaging structure. The red dashed line is the boundary between the scattering layer and the extinction layer. (e) SEM image of SiO_2 nanoparticles. The inset shows the particle size distribution with an average size of 136 nm. (f) SEM image of graphite nanoparticles. The inset shows the particle size distribution with an average size of 56 nm. (g) CIE chromaticity coordinates and color gamut (red line) of the mini-fc-LEDs. The inset shows normalized luminescence spectrum of the mini-fc-LEDs.

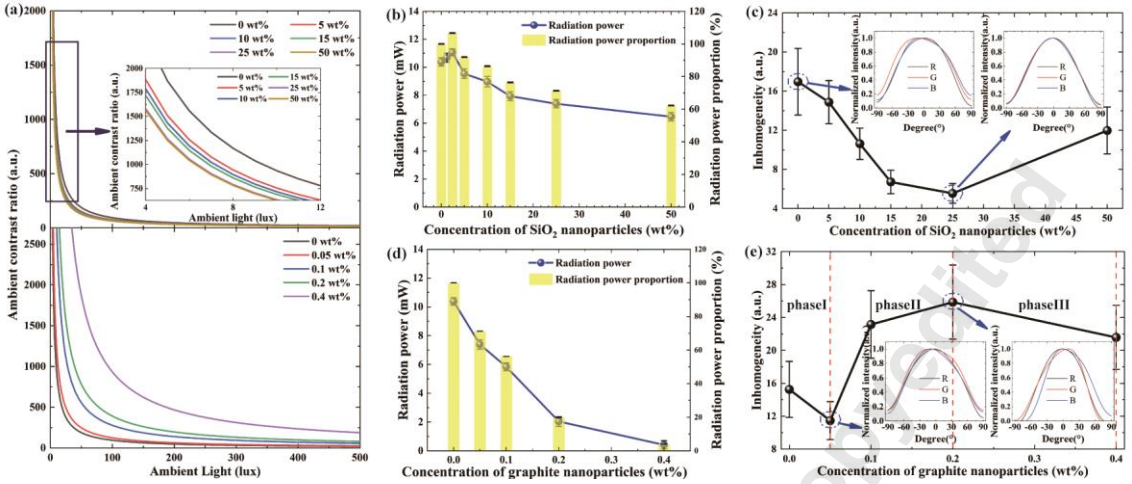

Figure 2. Effects of doped nanoparticles on the optical performances of SiO2-only devices and graphite-only devices. (a) Ambient contrast ratio (device brightness is 1500 nits) of device with different nanoparticle concentrations: upper, SiO2 nanoparticles; lower, graphite nanoparticles. The inset shows the details of Fig. 2. (a). (b) Radiation power of SiO2-only devices with different SiO2 concentration. (c) Inhomogeneity of SiO2-only devices with different SiO2 concentration. The inset shows the spatial light distribution curves of the red, blue, and green light corresponding to the degree of inhomogeneity. (d) Radiation power of graphite-only devices with different graphite concentration. (e) Inhomogeneity of graphite-only devices with different graphite concentration. In Fig. 2. (b) and (d), the radiation power proportion is the percentage of the SiO2-only devices/graphite-only devices relative to the conventional device.

Journal of Electronic Packaging. Received November 21, 2020;
Accepted manuscript posted February 16, 2021. doi:10.1115/1.4050202

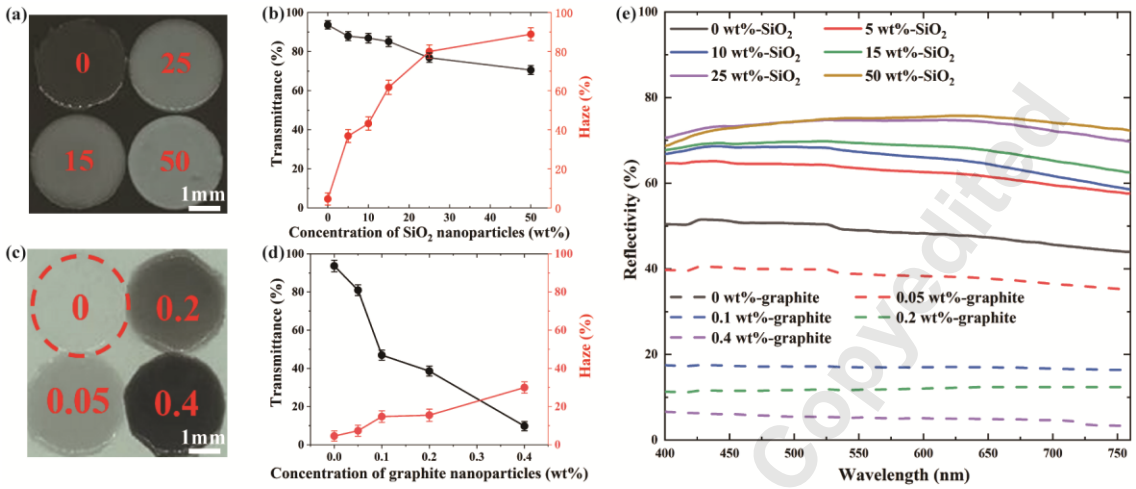

Figure 3. Effects of doped nanoparticles on the optical performances of films. (a) Photograph of SiO_2-only films with different SiO_2 concentration. (b) Transmittance and haze of SiO_2-only films with different SiO_2 concentration. (c) Photograph of graphite-only films with different graphite concentration. (d) Transmittance and haze of graphite-only films with different graphite concentration. (e) Visible light reflectance spectrum of SiO_2-only films (solid lines) and graphite-only films (dashed lines).

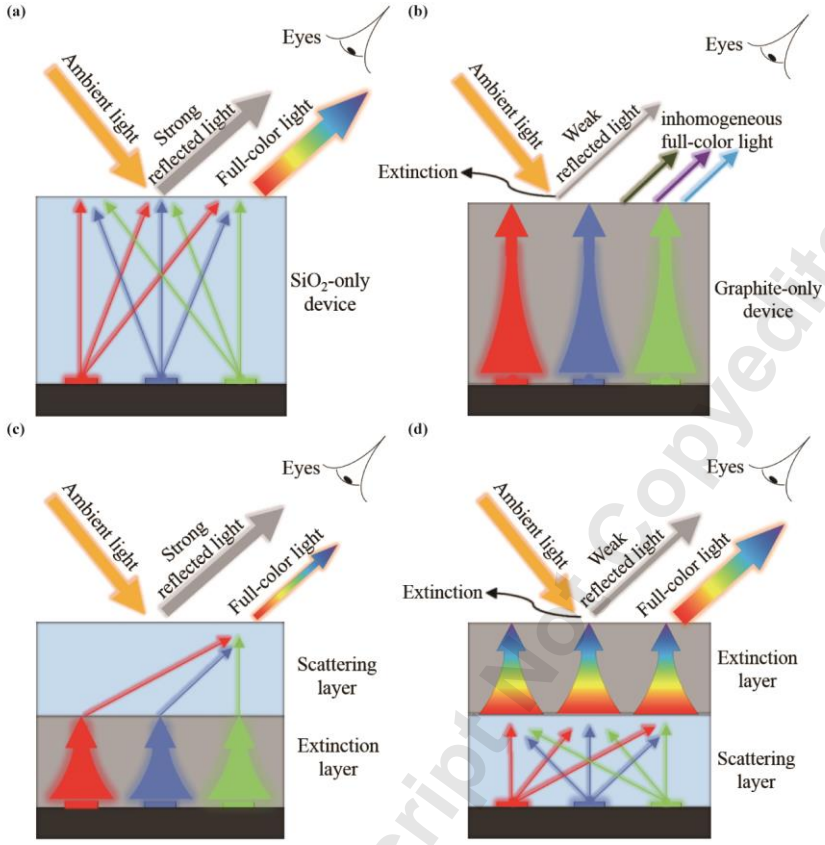

Figure 4. The structure and effect of different bi-layered devices. **(a)** The SiO_2-only device **(b)** The graphite-only device **(c)** The bi-layered device with a top scattering layer and a bottom extinction layer. **(d)** The bi-layered device with a top extinction layer and a bottom scattering layer.

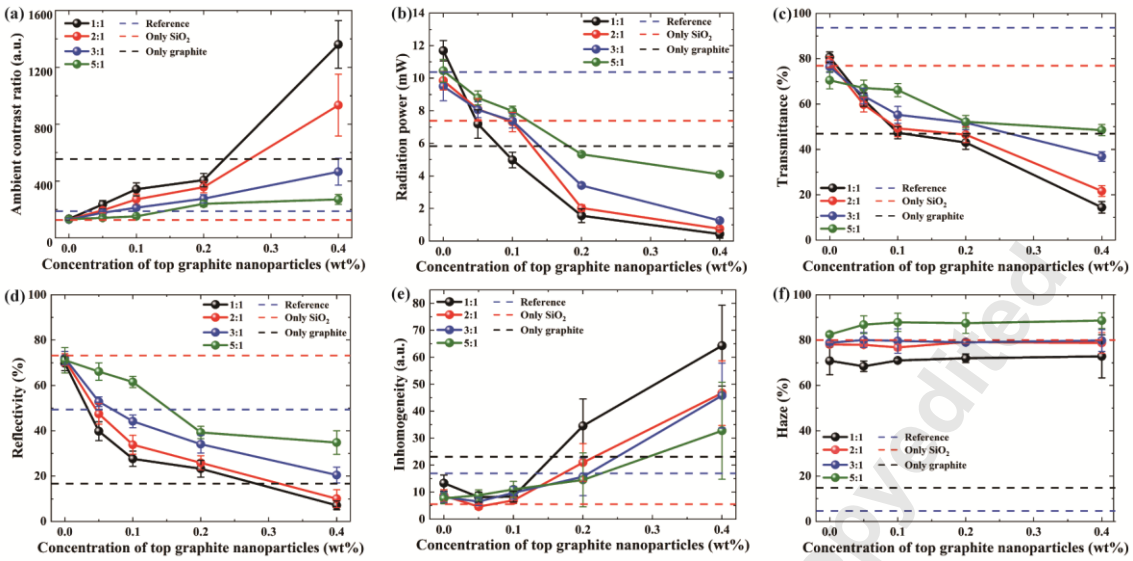

Figure 5. Effects of graphite concentration of top extinction layer and thickness ratio on the optical performances of bi-layered devices and bi-layered films. **(a)** ACR (device brightness is 1500 nits and the ambient brightness is 50 lux), **(b)** radiation power and **(d)** inhomogeneity of bi-layered devices with different graphite concentration and different thickness ratio. **(c)**Transmittance, **(e)** reflectivity and **(f)** haze of bi-layered films with different graphite concentration and different thickness ratio. In (a)-(f), the blue dashed line represents the performance of the conventional devices or films; the red dashed line represents the performance of the SiO_2-only device or films (SiO_2 concentration is 25 wt%); the blue dashed line represents the performance of the graphite-only device or films (graphite concentration is 0.4 wt%). All the SiO_2 concentration of the bottom scattering layer is 25 wt%; the thickness ratio refers to the value of the thickness of the scattering layer divided by the thickness of the extinction layer.

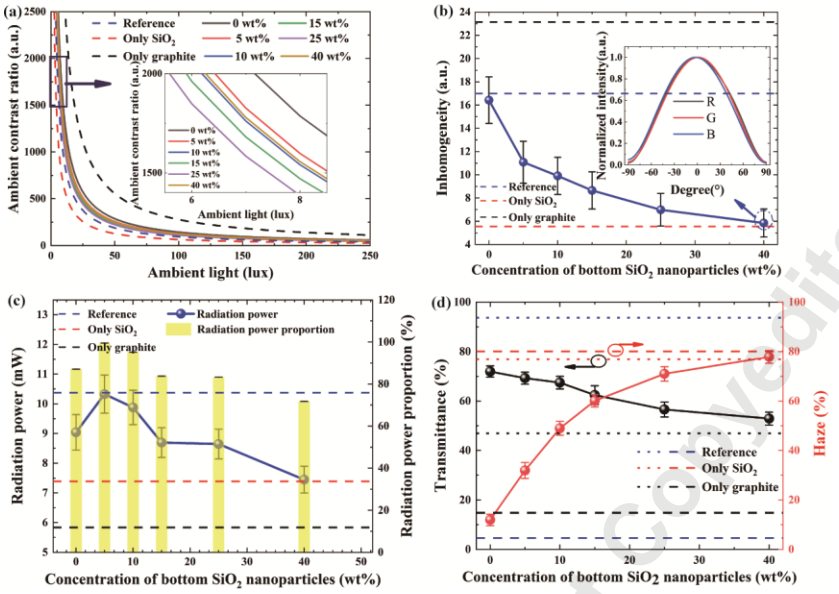

Figure 6. Effects of SiO_2 concentration on performance of bi-layered devices. **(a)** ACR (device brightness is 1500 nits), **(b)** inhomogeneity and **(c)** radiation power of bi-layered devices with different SiO_2 concentration. **(d)** Transmittance and haze of bi-layered films with different SiO_2 concentration. In (a)-(d), the blue dashed line represents the performance of the conventional devices or films; the red dashed line represents the performance of the SiO_2-only devices or films (SiO_2 concentration is 25 wt%); the blue dashed line represents the performance of the graphite-only devices or films (graphite concentration is 0.4 wt%). All the graphite concentration of top extinction layer is 0.1 wt% and the thickness ratio is 2:1.

Table 1 FOM of bi-layered devices with different graphite concentration and thickness ratio

Graphite concentration (wt%)	Thickness ratio 5:1	3:1	2:1	1:1
0	0.72	0.61	0.60	0.48
0.05	0.57	0.89	1.30（device A）	0.84
0.1	0.45	0.65	1.15（device B）	0.82
0.2	0.36	0.24	0.14	0.07
0.4	0.14	0.05	0.06	0.04

Table 2 Comparison of devices with different encapsulation structure

Devices	Radiation power (mW)		Inhomogeneity (a.u.)		ACR (device brightness: 1500 nits; ambient brightness: 50 lux)(a.u.)		FOM (a.u.)	
	Value	Growth	Value	Growth	Value	Growth	Value	Growth
Conventional devices	10.7	-30.8%	17.0	-65.9%	187.9	32.9%	0.48	168.8%
SiO_2-only devices (25 wt%)	7.3	0.01%	5.5	5.5%	127.4	96.1%	0.68	89.7%
Graphite-only devices (0.1 wt%)	5.8	27.6%	23.1	-74.9%	554.6	-54.9%	0.56	130.1%
Bi-layered devices (thickness ratio: 2:1; graphite concentration: 0.1 wt%;SiO_2 concentration: 40 wt%)	7.4	-	5.8	-	249.9	-	1.29	-